Chapter 5
MICROMECHANICAL MODELS FOR CONCRETE

5.1 INTRODUCTION

In this chapter three micromechanical models will be examined. The first two models are the differential scheme and the Mori-Tanaka model which predict the elastic modulus after the load is applied. The third model is a crack growth model which predicts the fracture of materials for a given initial pre-load system of cracks and different loading conditions. The experimental results presented in Chapter 4 will be compared to the theoretical models mentioned above.

5.2 ELASTIC MODULUS MODELS

There are several methods of predicting the effective macroscopic elastic moduli of a microscopically heterogeneous material. For the broad class of materials that consist of *inclusions* dispersed in a continuous matrix, the effective moduli depend on the moduli of the two components: the volumetric concentration of the inclusions, and the shape and orientation of the inclusions (Zimmerman 1991). Two of these methods are the differential scheme (McLaughlin 1977; Norris 1985) and the Mori-Tanaka (1973) method. Both models take the microgeometry of the materials into account for estimating the effect of pores and cracks on the elastic moduli. In concrete, the shapes of the inclusions can be estimated by two important idealized pore shapes, namely the sphere and the *penny-shaped* crack (Mehta and Monteiro 1993).

Both of these methods will be applied to predict the elastic modulus of concrete specimens under different loading conditions. The initial elastic modulus of each of the samples is obtainable from the stress-strain diagrams. In each experiment the loads were applied up to 90% of the ultimate strength, and the compressive stress-induced microcracks were preserved by injecting Wood's metal into the specimens while they were under sustained loads. For each experiment, the crack density was determined (see Chapter 4).

5.2.1 DIFFERENTIAL SCHEME

The effective macroscopic elastic moduli of a material can be predicted by means of two-dimensional and three-dimensional differential scheme analysis. Equation 5.1 is based on the two-dimensional analysis proposed by Salganik (1973):

$$E = E_0 e^{-\pi\Gamma_{2D}} \tag{5.1}$$

Equation 5.2 is based on the three-dimensional analysis (Zimmerman 1991):

$$E = E_0 e^{-16\Gamma_{3D}/9} \tag{5.2}$$

Where: E = Final elastic modulus

E_0 = Initial elastic modulus

Γ_{2D} = Crack density in two dimensions

Γ_{3D} = Crack density in three dimensions

The initial and final moduli of elasticity for Experiment #2, which is a uniaxial test, can be obtained from the stress-strain diagram:

$$E_0 = 2.625 \times 10^6 \text{ psi } (18.1 \times 10^3 \text{ MPa})$$

$$E = 2.375 \times 10^6 \text{ psi } (16.4 \times 10^3 \text{ MPa}).$$

From Table 4.3, the crack density for the uniaxial specimen is, Γ=0.0919; and for the reference (no-load) specimen, Γ=0.0444. The effective crack density is the difference between the crack density prior to and after the test. Hence, $\Delta\Gamma$=0.0475.

By applying Salganik's two-dimensional differential scheme solution (Equation 5.1), the final modulus of elasticity can be calculated:

$$E = 2.625 \times 10^6 \times e^{-\pi(0.0475)} = 2.261 \times 10^6 \text{ psi} \left(15.6 \times 10^3 \text{ MPa}\right)$$

Salganik's method produces a very accurate prediction of the modulus of elasticity, within 5% of the measured value.

Since the crack density measurements were performed in two dimensions, they should be converted to three-dimensional crack density for the three-dimensional differential scheme analysis (similar to Schlueter et al. 1991).

When a plane cuts through a concrete sample, it produces a section which contains line cracks. With respect to two-dimensional measurements, the length of these lines is considered to be the crack length, $2a$. However, in three-dimensional terms, these apparent lengths are not the true measurements of the cracks. Assuming the cracks in three dimensions are idealized to conform to the penny-shaped model shown in Figure 5.1, we can establish the relationship between the lengths of cracks in three dimensions ($2a_{act.}$) and their two dimensional lengths ($2a_{meas.}$).

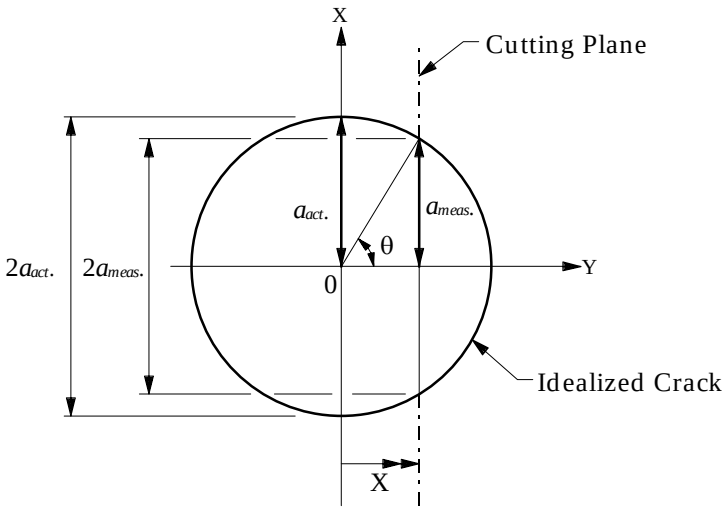

Figure 5.1 Schematic diagram of an idealized crack

For an idealized circular penny-shaped crack, we can write:

$$y^2 + x^2 = a_{act.}^2$$

or

$$y = \sqrt{a_{act.}^2 - x^2} = a_{meas.}$$

The mean value of $a_{meas.}$, $\overline{a_{meas.}}$, can be established from

$$\overline{a_{meas.}} = \frac{\int_0^{a_{act.}} \sqrt{a_{act.}^2 - x^2}\, dx}{\int_0^{a_{act}} dx = a_{act}}$$

Hence $$\overline{a_{meas.}} = \int_0^{a_{act.}} \sqrt{1 - \left(\frac{x}{a_{act.}}\right)^2}\, dx$$

let $\frac{x}{a_{act.}} = t$, then $dx = a_{act.} dt$. Substituting in the above equation,

$$\overline{a_{meas.}} = a_{act.} \int_0^1 \sqrt{1 - t^2}\, dt \tag{5.3}$$

But $$t = \frac{x}{a_{act.}} = \cos\theta$$

$$t^2 = \cos^2\theta$$

and $$1 - t^2 = \sin^2\theta$$

$$\sqrt{1 - t^2} = \sin\theta$$

Substituting the above in Equation 5.3 will yield:

$$a_{meas.} = a_{act.} \int_0^{\pi/2} \sin\theta \sin\theta d\theta = a_{act.} \int_0^{\pi/2} \sin^2\theta d\theta = a_{act.} \left(\frac{2\theta - \sin 2\theta}{4}\right) = \frac{\pi}{4} a_{act.}$$

$$a_{act.} = \frac{4}{\pi} a_{meas.} = 1.273 a_{meas.} \tag{5.4}$$

Equation 5.4 gives the actual length of a crack in three dimensional form as derived from the measured length in two dimensions. The two-dimensional and three dimensional crack densities were analyzed, and in some cases a relationship was developed between them (Hadley 1976; Batzle et al. 1980; Abdel-Gawad 1987; and He and Aherns 1994). However, the best result is given by stereological analysis, as explained below.

The number of cracks per unit volume, N_V, can be obtained from the following equation (Underwood 1968):

$$N_V = \frac{2N_A^2}{\pi N_L} \tag{5.5}$$

where N_A represents the number of cracks in two dimensions (Table 4.1) and N_L is the number of intersections of features, i.e. cracks, per unit length of test line (for more detail, refer to Chapter 3).

The crack radius, a, is defined as the ratio of the number of interceptions of features per unit length of test line, N_L, over the number of interceptions of features per unit test area, N_A (Underwood 1968). Therefore,

$$a = \frac{N_L}{N_A} \quad \text{or} \quad N_L = aN_A \tag{5.6}$$

Substituting Equation 5.6 in Equation 5.5 yields:

$$N_V = \frac{2N_A^2}{\pi(aN_A)} = \frac{2}{\pi}\frac{N_A}{a} \tag{5.7}$$

The three dimensional crack density is defined as:

$$\Gamma_{3D} = \frac{Na^3}{V} = N_V a^3 \tag{5.8}$$

substituting Equation 5.7 in Equation 5.8 gives:

$$\Gamma_{3D} = \frac{2N_A}{\pi a}a^3 = \frac{2}{\pi}N_A a^2 = \frac{2}{\pi}\Gamma_{2D} \tag{5.9}$$

Using Equation 5.9, the two-dimensional crack density can be converted to a three-dimensional one. Hence,

$$\Gamma_{3D} = \frac{2}{\pi}\Gamma_{2D} = \frac{2}{\pi}(0.0475)(1.273)^2 = 0.0490$$

The final elastic modulus can be estimated from Equation 5.2:

$$E = 2.625 \times 10^6 \times e^{-16(0.0490)/9} = 2.406 \times 10^6 \text{ psi } (16.6 \times 10^3 \text{ MPa})$$

The three-dimensional analysis result is 2% above the actual measured value. The two-dimensional analysis gives better results.

The initial and final effective moduli of elasticity for Experiment #5, which is a fully confined test, can be obtained from the stress-strain diagram:

$$E_0' = 1.875 \times 10^6 \text{ psi } (12.9 \times 10^3 \text{ MPa})$$

$$E' = 1.650 \times 10^6 \text{ psi } (11.4 \times 10^3 \text{ MPa}).$$

From Table 4.3, the crack density for the fully confined specimen is, Γ=0.0262; and for the reference (no-load) specimen, Γ=0.0444. The effective crack density is the difference between the crack density prior to and after the test. Hence, $\Delta\Gamma$=0.0182.

Applying Salganik's two-dimensional differential scheme solution (Equation 5.1), the final modulus of elasticity can be predicted as:

$$E_{Confined} = 1.875 \times 10^6 \times e^{-\pi(0.0182)} = 1.771 \times 10^6 \text{ psi } \left(12.2 \times 10^3 \text{ MPa}\right)$$

Salganik's method prediction of modulus of elasticity is within 10% of the measured value.

Converting the two-dimensional crack density into the three-dimensional one, using Equation 5.9 yields:

$$\Gamma_{3D} = \frac{2}{\pi}\Gamma_{2D} = \frac{2}{\pi}(0.0182)(1.273)^2 = 0.0188$$

The final elastic modulus can be estimated from Equation 5.2

$$E_{Confined} = 1.875 \times 10^6 \times e^{-16(0.0188)/9} = 1.813 \times 10^6 \text{ psi } (12.5 \times 10^3 \text{ MPa})$$

The three dimensional analysis result is 9% above the actual measured value.

5.3.1 THE MORI-TANAKA METHOD

Mori and Tanaka (1973) proposed the following equation to predict the elastic modulus of a material containing cracks:

Mori-Tanaka method: $$E = E_0/(1+\beta\Gamma) \tag{5.10}$$

where: $\beta = 16(10-3\nu_0)(1-\nu_0^2)/45(2-\nu_0)$

and ν_0 = Poisson's ratio

For concrete, typically ν_0 = 0.20, so:

$$\beta = 16[10-3(0.20)](1-0.20^2)/45(2-0.20) = 1.78$$

and for the Mori-Tanaka method:

$$E = \frac{2.625\times10^6}{1+(1.78)(0.0768)} = 2.309\times10^6 \text{ psi } (15.9\times10^3 \text{ MPa})$$

The modulus of elasticity predicted by the Mori-Tanaka model is within 3% of the measured value. For the fully confined specimen,

$$E_{Confined} = \frac{1.875\times10^6}{1+(1.78)(0.0182)} = 1.816\times10^6 \text{ psi } (12.5\times10^3 \text{ MPa})$$

The predicted modulus of elasticity is within 10% of the measured value for the fully confined condition.

Table 5.1 represents the summary of the predicted modulus of elasticity obtained from the differential scheme and Mori-Tanaka method.

Table 5.1 Modulus of elasticity obtained from micromechanical Models

Concrete Specimen	Measured E	2D Differential	3D Differential	Mori-Tanaka Method
Uniaxial	2.375×10^6 psi (15.6×10^3 MPa)	2.261×10^6 psi (15.6×10^3 MPa)	2.406×10^6 psi (16.6×10^3 MPa)	2.309×10^6 psi (15.9×10^3 MPa)
Confined	1.650×10^6 psi (11.4×10^3 MPa)	1.771×10^6 psi (12.2×10^3 MPa)	1.813×10^6 psi (12.5×10^3 MPa)	1.816×10^6 psi (12.5×10^3 Pa)

The differential scheme and the Mori-Tanaka model consider the change in the overall moduli when a small increment of the inclusion phase is introduced in a material. The corresponding change in the field variables is neglected by the Mori-Tanaka model, whereas in the differential scheme the change in the field variables is related to the change of the volume fraction of the inclusion. It has been shown that, as the volume fraction goes to zero, the two methods agree asymptotically, although their specific predictions may be different, depending on the problem (Nemat-Nasser and Hori 1993).

5.3 CRACK GROWTH SIMULATION MODEL

Du (1994) has developed a micromechanical model by which, given the initial crack conditions in an unloaded specimen, the final cracking state can be predicted for different loading conditions. The experimental results obtained and discussed in Chapter 4 will be compared to the theoretical results obtained using Du's crack-growth model.

Du's model employs three commonly used fracture criteria. They are:

a) The maximum stress criterion, σ-criterion;

b) The maximum energy release rate criterion, G-criterion;

c) The minimum strain energy density criterion, S-criterion.

The criterion most commonly used for concrete is the maximum energy release rate criterion.

5.3.1 The Maximum Energy Release Rate Criterion, G-Criterion

The energy release rate is usually defined as the energy released from the body per unit crack advance. A more precise definition (Moran and Sih 1987) involves the work input into the crack tip. Irwin (1956) defined an energy release rate, G, which is a measure of the energy available for an increment of crack extension. Considering the plate, shown in Figure 5.2, with a thickness B, and containing a crack with a length of $2a$.

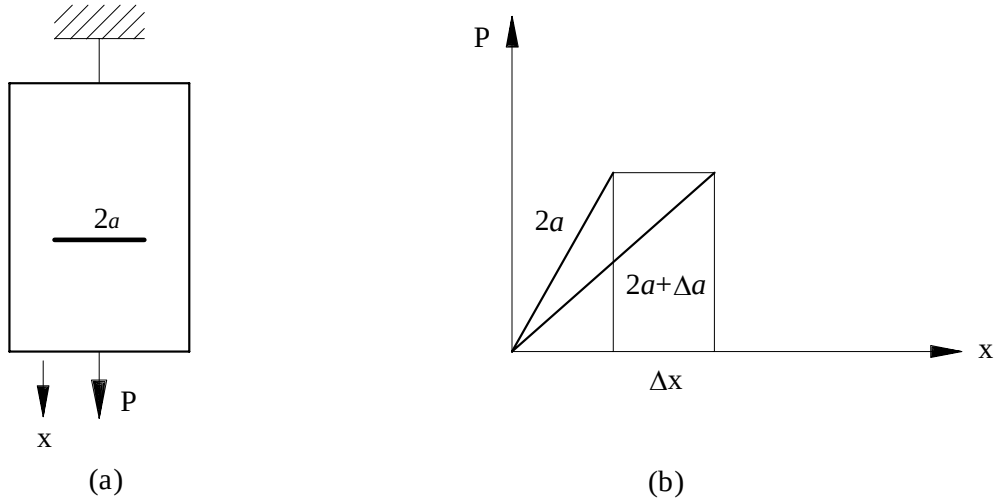

Figure 5.2 (a) Plate with crack $2a$; (b) Load-displacement diagram

If the plate is subjected to a constant load P, the energy released can be expressed by crack growth Δa as (Mehta and Monteiro 1993):

$$GB\Delta a = P\Delta x - \Delta U_e$$

where ΔU_e is the change in elastic energy due to crack growth Δa. In the limit:

$$GB = P\frac{dx}{da} - \frac{dU_e}{da} \tag{5.11}$$

the strain energy U_e in terms of compliance is given by:

$$\Delta U_e = \frac{cP^2}{2}$$

and Equation 5.11 becomes:

$$G = \frac{P^2}{2B}\frac{dc}{da} \tag{5.12}$$

Where: G = energy release rate

P = applied load

B = plate thickness

c = compliance (displacement/load)

a = half-crack length

Irwin (1957) defined the quantity G_c as the work required to produce a unit increase in crack area, referred to as *critical energy release rate.* G_c is a material property and is determined experimentally. In order to determine whether or not a crack will propagate, the value of energy release per unit increase crack area, G, is computed. If the energy release rate is lower than the critical energy release rate ($G < G_c$), the crack is stable. Conversely, if $G > G_c$, the crack will propagate. A condition in which the energy release rate equals the critical energy release rate ($G = G_c$) is known as metastable equilibrium.

The stress intensity factor, K_I, is defined as:

$$K_I = \sigma\sqrt{a}\, f(g) \tag{5.13}$$

Where: K_I = stress intensity factor for mode I (stress $\sqrt{\text{length}}$)

σ = applied stress

$f(g)$ = a function depending on the specimen and crack geometry

These two parameters, the energy release rate and the stress intensity factor, describe the behavior of cracks. The former quantifies the net change in potential energy that accompanies an increment of crack extension; the latter characterizes the stresses, strains, and displacements close to the crack tip. The energy release rate describes global behavior, whereas the stress intensity factor is a local parameter. For linear elastic materials, K_I and G_c are uniquely related. Considering only mode I and plane stress condition, for linear elastic behavior:

$$G = \frac{K_I^2}{E} \tag{5.14}$$

The *critical stress intensity factor*, K_c, commonly known as *fracture toughness,* is assumed to be a material property.

The G-criterion, usually called the maximum energy release rate, states that:

a) Crack initiation takes place at the crack tip and in a direction with respect to the original crack plane.

b) Crack extension takes place in the direction along which the strain energy release rate is maximum.

c) Crack initiation occurs when the maximum strain energy release rate in a direction reaches a critical value.

5.3.2 Crack Growth and propagation

The Du model uses the displacement discontinuity method which allows the fracture mechanics parameters to be readily computed for a given crack problem. By assuming a virtual crack increment, the crack initiation direction can be determined by one of the three fracture initiation criteria discussed in the previous section. The crack propagation path can be determined by assuming several crack increments. After each crack increment, the computer program recalculates the fracture parameters and the corresponding initial angle of crack propagation is determined. Figure 5.3 is the flow chart of the Du model computer program.

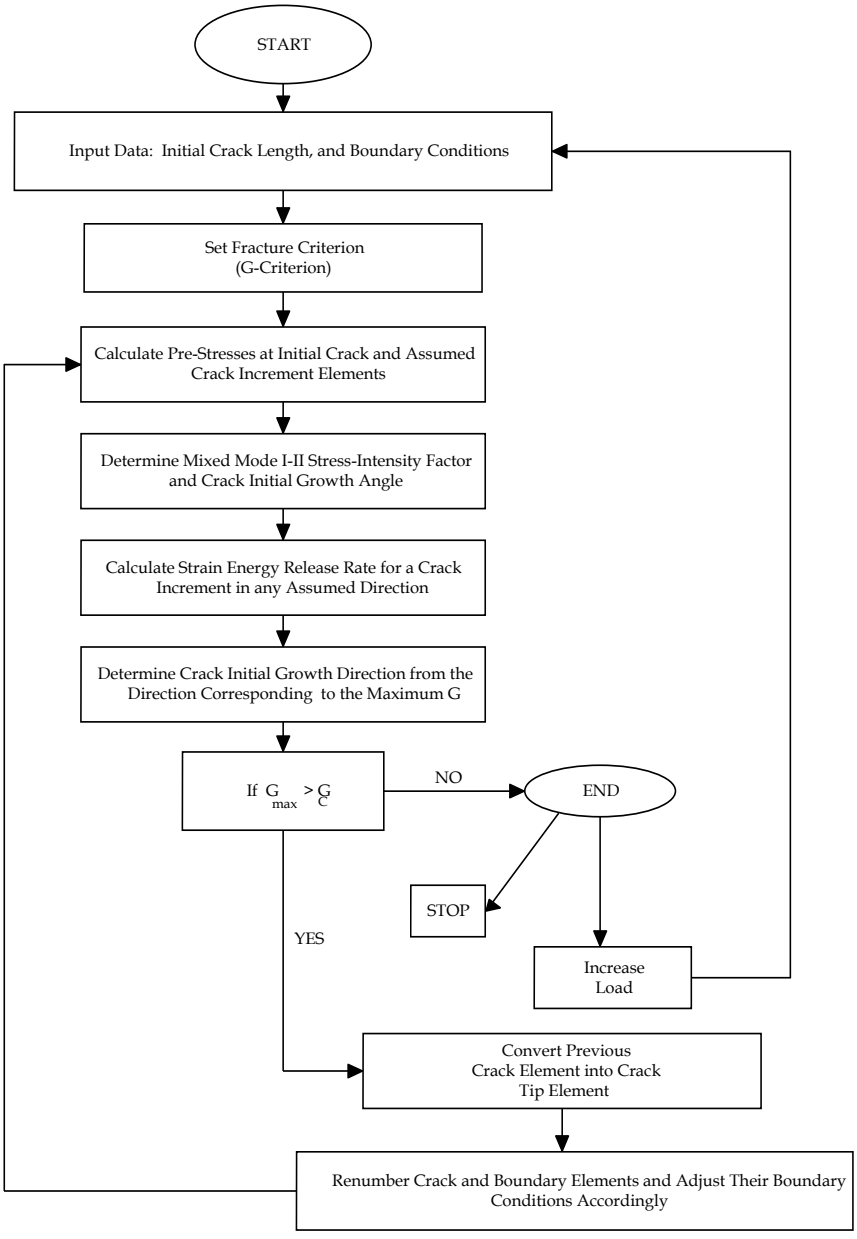

Figure 5.3 Computer flow chart for the Du model calculations

5.3.3 Review of Analytical Micromechanical Model

The purpose of the Du model is to numerically simulate the behavior of stochastic distributions of heterogeneous microcracks. This behavior is difficult to model using analytical models. Du's micromechanical model is based on the idea that frictional sliding along pre-existing cracks results in the formation of tension cracks at their tips. The basis for the model is the *displacement discontinuity model* of Crouch and Starfield (1983). This model is based on the analytical solution to the problem of a constant discontinuity in displacement over a finite line segment in the x,y plane on an infinite elastic solid. A displacement discontinuity can be visualized physically as a line crack whose opposing surface have been displaced relative to one another. In the case under consideration here, surfaces are displaced relatively by a constant amount along the entire crack. However, in general, one could consider an arbitrary distribution of relative displacement.

This method is based on the notion that one can make a discrete approximation of a continuous distribution of displacement discontinuity along a crack. That is, a crack can be divided into a series of N elements (boundary elements) and the displacement discontinuity assumed to be constant over each one. On the basis of the analytical solution for a single, constant element displacement discontinuity, we derive a numerical solution to the problem by summing up the effects of all N elements. When the distribution of displacement discontinuity along the crack is not known, the distribution of traction applied to the crack surfaces must be known in order to define the problem properly. The values of the element displacement discontinuities necessary to produce these tractions, are then sought, element by element along the crack (Crouch and Starfield 1983).

5.3.4 Distribution of Microcracks in the Material

The microcracks yielded by Experiment #1, the no-load experiment, were used as the initial input microcracks in the Du model. Figure 5.4 is the histogram of the microcracks in that experiment.

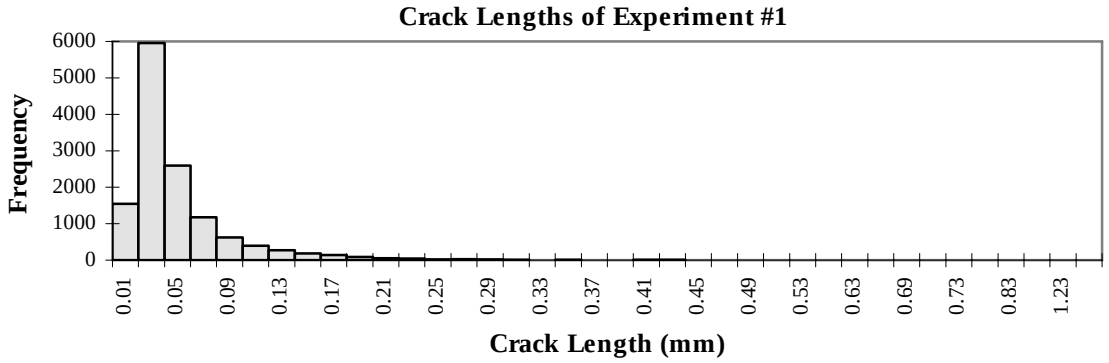

Figure 5.4 Histogram of entire microcrack length distribution for the no-load experiment on normal-strength concrete

Table 5.2 is the tabulation of the microcracks used in the model.

Table 5.2 The microcrack lengths used in the Du model

NORMAL-STRENGTH CONCRETE	
Crack Length (mm)	**Frequency**
0.4	26
0.5	18
0.6	4
0.7	4
0.8	3
0.9	1
1.0	1
1.3	1
1.5	1
Total	59

Crack lengths smaller than 0.4 mm are ignored and, because crack apertures are negligibly small, line cracks were assumed.

The Du model uses the Monte Carlo technique to generate a distribution of line cracks. Monte Carlo simulation is used for problems involving random variables with known (or assumed) probability distribution.

Because of the assumption of a uniformly random distribution of initial crack locations and orientation, an algorithm has been developed to generate a similar distribution. For each crack generated, three random numbers are initially picked to determine the crack position (x,y), orientation, and according to Table 5.2, a non-random crack generation is implemented to generate a distribution of crack length L (Kemeny 1991). The crack orientations are between 0° and 90°. A tree-cutting algorithm is used to eliminate cracks that intersect. Figure 5.5 is an illustration of the cracks generated in a concrete specimen with rectangular boundaries.

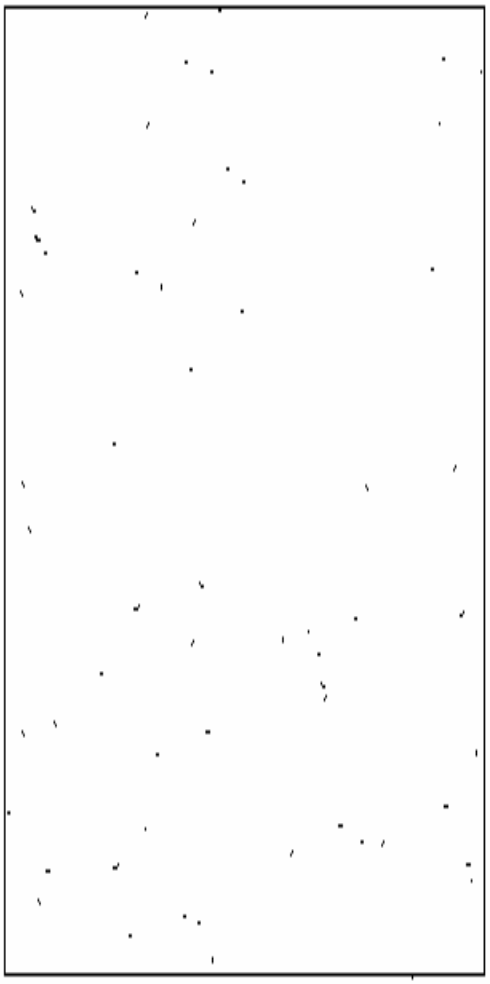

Figure 5.5 The random cracks generated in concrete specimen

5.3.5 Parameters Used in the Crack Growth Model

The CEB-FIP model code 1990 recommends the use of the following expression for the energy release rate:

$$G_f = \alpha_f \left(f_{cm} / f_{cmo} \right)^{0.7} \tag{5.15}$$

where α_f is a coefficient which depends on the maximum aggregate size d_{max}, which for 3/8 inch (10 mm) MSA is 0.02 Nmm/mm^2, and f_{cmo} is equal to 10 MPa (Mehta and Monteiro 1993). f_{cm} is the average 28-day compressive strength. The strength data that is available is the strength after more than 2 years (840 days). In order to obtain the 28-day compressive strength of the concrete specimen, the CEB-FIP model code (1990) suggests the following relationship:

$$f_{cm}(t) = \exp\left[s\left(1 - \left(\frac{28}{t/t_1} \right)^{1/2} \right) \right] f_{cm} \tag{5.16}$$

where $f_{cm}(t)$ = mean compressive strength at age t days

f_{cm} = mean 28-day compressive strength

s = coefficient depending on the cement type, such as s=0.25 for normal hardening cement

t_1 = 1 day

$$51.7 \text{ MPa } (7{,}500 \text{ psi}) = \exp\left[0.25\left(1 - \left(\frac{28}{840} \right)^{1/2} \right) \right] f_{cm}$$

$$f_{cm} = 42.14 \text{ MPa } (6{,}100 \text{ psi})$$

By substituting in equation 5.15,

$$G_f = \left(0.02 \times 10^3 \text{ Nm}^{-1} \right) \left(\frac{42.14 \text{ MPa}}{10 \text{ MPa}} \right)^{0.7} = 54.7 \text{ Nm}^{-1}$$

Irwin (1957) showed that the energy release rate and the stress intensity factor approaches are equivalent. For linear elastic behavior, considering only mode I and plane stress condition:

$$G_I = \frac{K_I^2}{E} \tag{5.17}$$

For E=2.625×10^6 psi (18.1 GPa),

$$K_I = \sqrt{G_f.E} = \sqrt{(54.7\ \text{Nm}^{-1})(18.1\times10^9\ \text{Pa})} \approx 1\ \text{MPa}\sqrt{\text{m}}$$

A Poisson's ratio, ν, value of 0.2, and a coefficient of friction, μ, value of 0.35 are assumed for the concrete specimen. The representative parameter values for the concrete specimen are shown in Table 5.3:

Table 5.3 Material properties for Concrete specimen

Crack Orientation	Random
Crack Location	Random
Crack Length, $2a$	0.4-1.5 mm
Poisson's Ratio, ν	0.2
Young's Modulus, E	18.1 GPa
Fracture Toughness, K_{IC}	1 MPa $\sqrt{\text{m}}$
Crack Density, Γ	0.0444
Friction Coefficient, μ	0.35
Crack Initial Angle, θ	4.9°

All representative parameter values for concrete were taken from Table 5.3 except the crack lengths which were taken from Table 5.2. Figure 5.6 shows the concrete specimen's cross section with the boundary dimensions for the input algorithm.

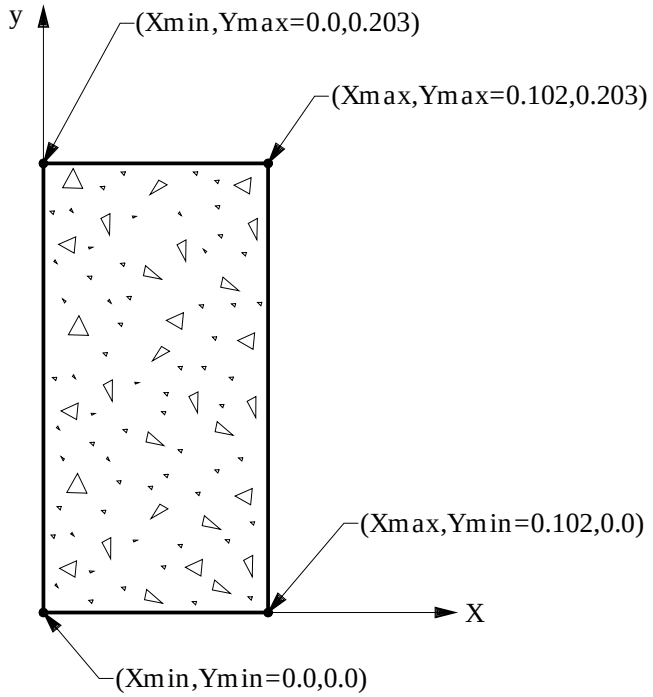

Figure 5.6 Concrete specimens boundary input in algorithm

The algorithm above generates the crack pattern, which represents the preload cracking status.

5.3.6 Program Overview

As mentioned earlier, the Du model was developed by making a series of modifications to the code of the displacement discontinuity method of Crouch and Starfield (1983). The computer program is called MCPP (Multiple Crack Propagation Program). It is a two dimensional boundary element code which simulates the multiple crack growth, interaction, and coalescence in materials. MCPP is a command-driven (rather than menu-driven) computer program.

The input file is prepared from the rectangular boundary of the concrete specimen's cross section, shown in Figure 5.7, and its information is kept in a file named *Bouninput.dat1*.

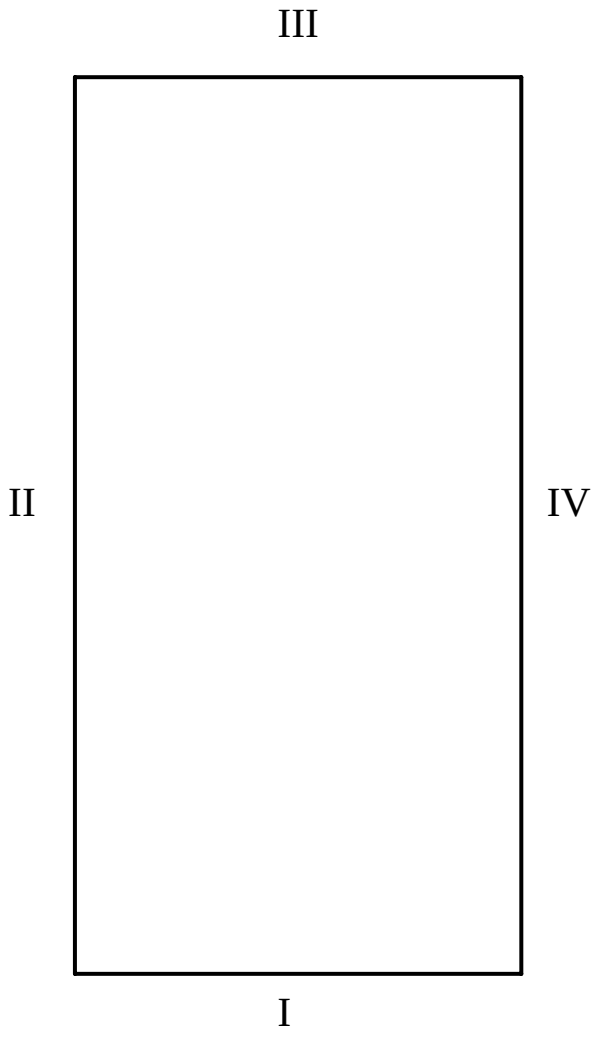

Figure 5.7 Rectangular boundary

The parameters which are read into the program from *Bouninput.dat1* are:

Numbs, Xlow, Ylow, Xlow, Yhigh, An low, An high, Kode, BVS, BVN, Al low, Al.high.

Where *Numbs* = number of straight line boundary segment used to define boundary contours.

(*Xlow, Ylow*) and (*Xhigh, Yhigh*) are the beginning and ending coordinates of boundaries I, II, III, IV.

Kode = 1 indicates that σ_s and σ_n are prescribed.

BVS = resultant shear strength (σ_s) or shear displacement (u_s)

BVN = resultant normal-strength (σ_n) or normal displacement (u_n)

An low = minimum angle = 0°

An High = maximum angle =180°

Al low = minimum crack length

Al High = maximum crack length

For program running procedures, refer to Appendix B.

5.3.7 The Crack Growth Simulation Model Results

Using the random crack distribution shown in Figure 5.5, and employing the Du model, with the axial displacement of 0.00001 meters for 50 iteration, will produce the image shown in Figure 5.8. The material properties used are tabulated in Table 5.3. The material in the model was subjected to an axial strain of 0.25%.

$$\left(\varepsilon_a = \frac{(0.00001\,\text{meter})(50\,\text{iterations})}{0.203\,\text{meter}} = 0.0025 = 0.25\%\,\text{strain} \right)$$

The crack density in Figure 5.8 was measured to be $\Gamma_{uniaxial} = 0.2173$.

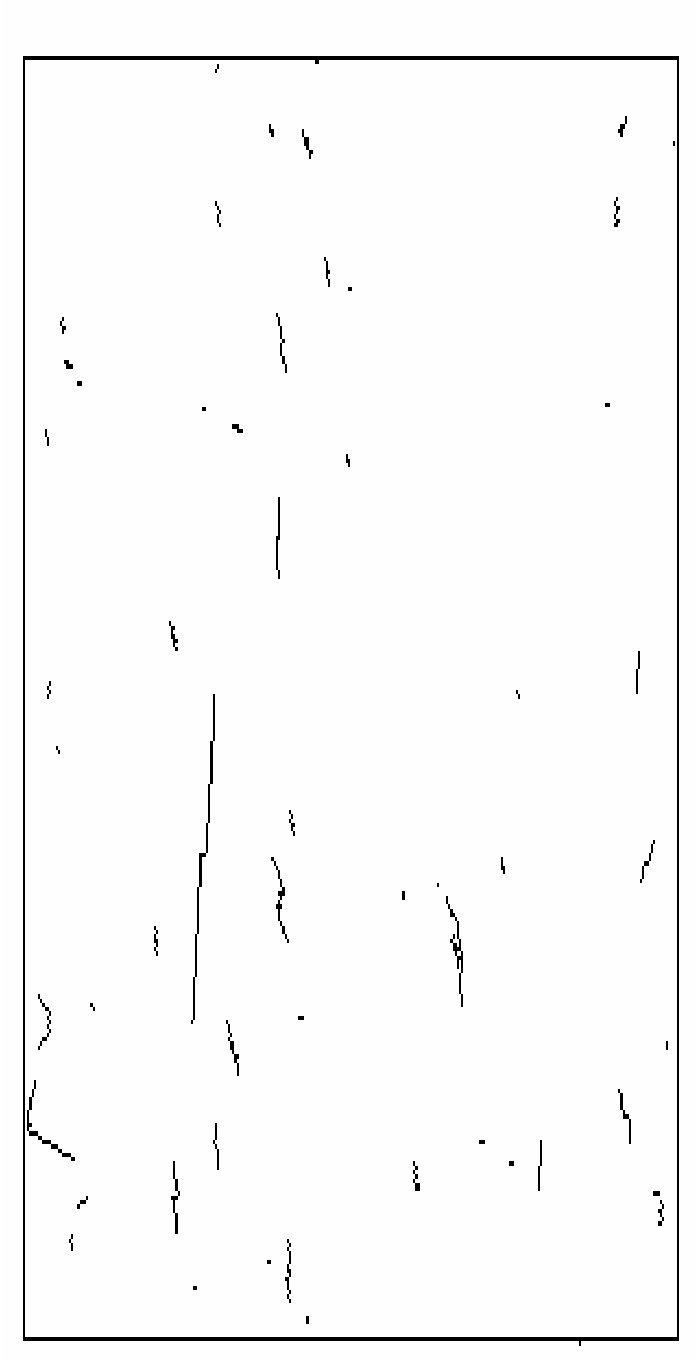

Figure 5.8 Crack propagation simulation for uniaxial loading

The same no-load model in Figure 5.5 was then subjected to a confined test, with the same number of iteration and axial strain. The result is shown in Figure 5.9. It is evident that the number of cracks propagating from the original cracks, and also the number of post-load generated cracks was reduced. The resulting

crack density was measured to be $\Gamma_{confined} = 0.1878$. There was about 15% reduction in crack density due to presence of confining stress.

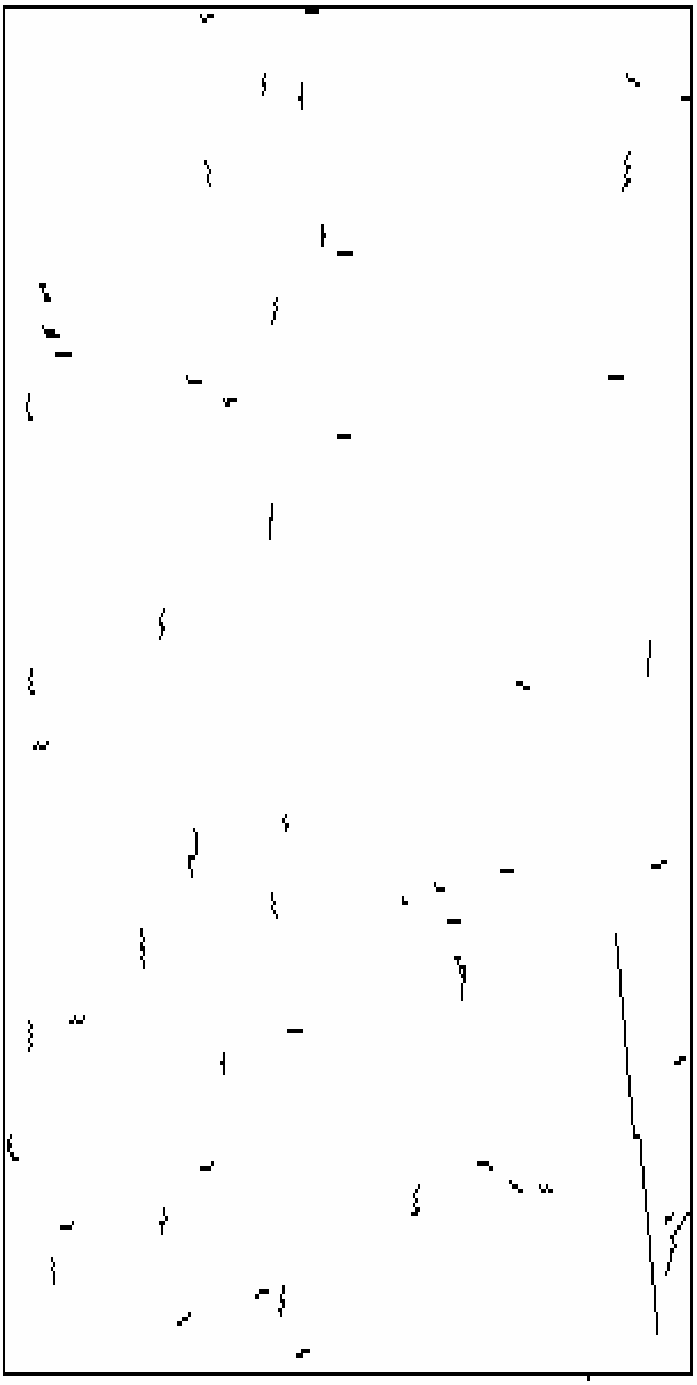

Figure 5.9 Crack propagation simulation for fully confined condition

The Du model results are consistent with the experimental results which were presented in Chapter 4. The experimental results showed that the crack density reduced when confining stress was used. The Du model also showed the same behavior. Experimental measurements indicated that the average crack length distribution strongly depends on the confining stress. The results obtained from the Du model, also indicates that the average crack length decreased when confinement was used. Most cracks in the Du model have an orientation subparallel to the direction of maximum applied stresses. The definite crack orientation in the Du model is due to the fact that there are no aggregates in the model and it is similar to testing a mortar specimen. The application of the Du model to concrete crack growth simulation should be enhance to include hard inclusions, i.e. aggregates, in the model.